ARTICLES

The Pulse of Calm Fan Deltas

Wonsuck Kim and Douglas J. Jerolmack[1]

Department of Civil and Environmental Engineering and Department of Geology, University of Illinois, Urbana-Champaign, Illinois 61801, U.S.A.; and National Center for Earth-surface Dynamics, University of Minnesota, Minneapolis, Minnesota 55414, U.S.A.
(e-mail: geowskim@uiuc.edu)

ABSTRACT

At the heart of interpreting the history of Earth surface evolution preserved in the rock record is distinguishing environmental (allogenic) forcing from internally generated (autogenic) "noise." Allogenic deposits classically have been recognized by their cyclic nature, which apparently results from periodic changes in base level, sediment supply, or tectonics. Autogenic deposits, which are quite variable in their origin and scale, are caused by the nonlinearity of sediment transport and might be expected to have a random or scale-free (fractal) signature. Here we describe a robust mechanism that generates cyclic deposits by an autogenic process in experimental fan deltas. Sheet flow over the fan surface induces deposition and an increase in fluvial slope and curvature to a point where the surface geometry is susceptible to a channelization instability, similar to channel initiation on hillslopes. Channelized flow results in incision and degrading of the fan surface to a lower slope, releasing a pulse of sediment that pushes the shoreline forward. Sheet flow resumes once the surface is regraded, and the cycle repeats in a surprisingly periodic fashion to produce cyclic foreset accretions. We use simple scaling and a one-dimensional fan evolution model to (1) demonstrate how time-varying flow width can cause pulses in sediment discharge at the shoreline in agreement with experiments and (2) reinterpret cyclic deposits reported in the field. Alternating sheet and channelized flows are known to operate on noncohesive fans in nature. Our results suggest that rather than reflecting variation in environmental forcing, many observed cyclic sedimentation packages may be a signature of the autogenic "pulse" of fan deltas under calm environmental conditions.

Online enhancement: appendix.

Introduction

Conservation of mass dictates that erosion and deposition are the result of spatial variation in sediment discharge. The presence of sedimentary bodies bounded by surfaces of erosion or non-deposition is the record of variation in sediment supply, water supply, or transportability (i.e., applied stress), which indicates unsteadiness in sediment transport. The recognition of cycles of depositional environments in the stratigraphic record precipitated an active line of research to unravel the nature and source of such unsteadiness (Pitman 1978; Blair and Bilodeau 1988; Posamentier et al. 1988; Smith 1994; Dorsey et al. 1997; Cui et al. 2003). There arose a general agreement that ubiquitous, repetitive packages of erosion and deposition result from large-scale climate change (e.g., Milankovich cycles; Imbrie et al. 1984) or tectonic change that affected sediment supply (e.g., Blair and Bilodeau 1988; Colella 1988; Price and Scott 1991; Dorsey et al. 1997; Gupta et al. 1999; Dorsey and Umhoefer 2000) and/or base level (e.g., Posamentier et al. 1988). Associating depositional sequences with allogenic changes in environmental controls allowed for correlation of sedimentary units around the globe (e.g., Haq et al. 1987; Posamentier et al. 1988) and quantitative reconstruction of Earth's climate and tectonic history (e.g., Paola 2000 and references therein).

Although climate change appears to be quasi-periodic and climatic cycles are expected to induce changes in sedimentation, work in recent decades has revealed richness in the stratigraphic record that complicates the above picture. Several authors

Manuscript received September 27, 2007; accepted March 20, 2008.

[1] Department of Earth and Environmental Sciences, University of Pennsylvania, Philadelphia, Pennsylvania 19104, U.S.A.; and National Center for Earth-surface Dynamics, University of Minnesota, Minneapolis, Minnesota 55414, U.S.A.

[The Journal of Geology, 2008, volume 116, p. 315–330] 0022-1376/0000/11604-0001$15.00 DOI: 10.1086/588830

have recognized the statistical signature of randomness in some deposits and questioned the apparent cyclicity reported in the literature (Drummond and Wilkinson 1993, 1996; Drummond et al. 1996; Wilkinson et al. 1998; Diedrich and Wilkinson 1999). Numerical models incorporating some degree of randomness have succeeded in describing many aspects of depositional sequences without invoking climate cycles (Sadler and Strauss 1990; Drummond and Wilkinson 1993; Jerolmack and Sadler 2007) and provide a powerful null hypothesis against which to test the control of climate. Detailed analysis of the rock record has also revealed acyclic but nonrandom statistics that are not explicable by either periodic climate cycles or purely random variability (Rothman et al. 1994; Pelletier and Turcotte 1997; Jerolmack and Sadler 2007).

Positing a direct relationship between environmental controls and sediment transport responses implies that the sediment transport system is (1) linear and (2) in equilibrium with imposed boundary conditions. Fluvial sediment transport may indeed be approximated as a linear process when averaged over the appropriate time and space scales (e.g., Howard 1982; Paola et al. 1992; Paola 2000). In such cases, the timescale of a purported environmental perturbation may be compared with the response time of the system (as determined by sediment transport rate and system size) to determine the likelihood of a 1 : 1 relationship between forcing and response (e.g., conventional stratigraphy; Mackin 1948; Jervey 1988; Posamentier et al. 1988). Several studies have noted that the diffusive nature of depositional fluvial regimes acts to attenuate high-frequency environmental signals and, hence, damp climate/tectonic fluctuations at timescales that are smaller than the system response time (Ellis et al. 1999; Allen and Densmore 2000; Castelltort and Van Den Driessche 2003; Swenson 2005). In addition, the response time of sedimentary systems may be long (tens to hundreds of k.yr.), challenging the notion that high-frequency climate or tectonic signals are preserved in the stratigraphic record (Castelltort and Van Den Driessche 2003; Jerolmack and Sadler 2007; Kim and Paola 2007).

At what point does the assumption of linearity and steadiness in sediment transport break down? It has been recognized for some time that a river does not steadily convey sediment downstream but rather pulses sediment by alternation of storage and release events (Leopold et al. 1964; Bull 1977; Gomez et al. 2002). Recent research has begun to focus on the inherent variability of sediment transport itself as a source of unsteadiness capable of generating depositional units at a variety of scales (Rothman et al. 1994; Gomez et al. 2002; Jerolmack and Mohrig 2005; Jerolmack and Paola 2007; Jerolmack and Sadler 2007). The statistical signature of autogenic processes, as measured by the distribution of thicknesses of sedimentary bodies, has been characterized as either exponential (the result of randomness; Paola and Borgman 1991; Drummond and Wilkinson 1996; Pelletier and Turcotte 1997; Wilkinson et al. 1998) or power law (the result of nonlinear dynamics; Rothman et al. 1994; Gomez et al. 2002). Autogenic variability may dominate the stratigraphic record over timescales up to hundreds of thousands of years (Jerolmack and Sadler 2007).

The picture that emerges from these studies is that autogenic fluctuations may generate acyclic deposits at timescales that are smaller than the response time of the system, while allogenic forcing creates large, cyclic (e.g., periodic in space) depositional sequences at longer times. There are observations, however, of small-scale cyclic deposits that do not fit neatly into either of these categories. Particularly common are cyclic fan sequences, which have been attributed to high-frequency sea level fluctuations (Amorosi et al. 2005), earthquake clustering (Dorsey et al. 1997), and/or episodic tectonic subsidence (Colella 1988). The relatively short timescales inferred from these deposits, 1–10 k.yr., calls into question whether they could possibly reflect allogenic forcing in a straightforward way (Castelltort and Van Den Driessche 2003). In this article, we describe regularly recurrent (cyclic) sedimentary packages caused by an autogenic process at relatively short timescales, using results from recent experiments at the Experimental EarthScape facility in the St. Anthony Falls Laboratory, University of Minnesota (Kim et al. 2006*a*, 2006*b*; Kim and Paola 2007). Evolution of the experimental fan delta using a noncohesive sediment mixture exhibits periodic fluctuations in mean shoreline position under steady boundary conditions that result from basinwide storage and release of sediment on the fluvial surface (Kim et al. 2006*a*). We propose that alternation between sheet flow and channelized flow causes regular fluctuations in the fluvial slope, and we demonstrate via a one-dimensional morphodynamic model that this mechanism generates periodic foreset sequences in agreement with experimental stratigraphy. This mechanism appears to be robust, with a cycle period that scales with sediment discharge and magnitude of fluvial slope variation. Scaling up to the size of field observations suggests that at least some cyclic sequences associated with fan deposits

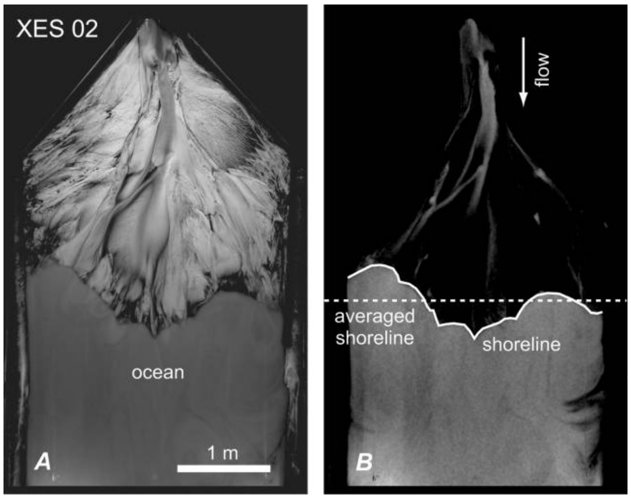

Figure 1. *A*, Overhead image taken during the initial base-level stable stage in XES 02. *B*, Flow map contrasting wet and dry portions on the fluvial surface. The solid line indicates a digitized shoreline, and the dotted line indicates a laterally averaged shoreline. A color version of this figure is in the online edition of the *Journal of Geology*

may be generated by this autogenic "pulse" of fluvial systems.

Experimental Setting

The Experimental EarthScape (XES) facility has been described in previous articles (Paola 2000; Paola et al. 2001), so only a brief summary is presented here. Data are taken from early stages of two XES experiments conducted in 2002 (henceforth XES 02) and 2005 (XES 05), under conditions of stable base level. Details of each experiment can be found in work by Kim et al. (2006*a*, 2006*b*) for XES 02 and Kim and Paola (2007) for XES 05. The XES basin has a working section that is approximately 3 m wide and 6 m long and a subsiding basement up to 1.5 m deep (fig. 1*A*). Experimental controls for both experiments are summarized in table 1.

The experimental sediment was composed of a mixture of white quartz sand and black coal sand. The coal has a specific gravity of 1.3, whereas quartz has a specific gravity of 2.65, so the coal grains were substantially more mobile than quartz grains and thus served as a proxy for fine-grained clastics. This sediment was premixed with water and introduced into the experimental basin at a point source located in the center of the upstream end (fig. 1*A*). Differences between the two experiments analyzed here were (1) total sediment and water discharge and (2) base-level and subsidence settings. Experiments XES 02 and XES 05 had a comparable sediment-water ratio, but XES 05 had a total discharge that was approximately five times lower than that of XES 02 (table 1). Experiment XES 02 can be characterized as having a strong base-level control in stratal development through time-varying base level (Kim et al. 2006*a*, 2006*b*), while XES 05 was designed to demonstrate the control of lateral variation in subsidence rate on stratigraphy (Kim and Paola 2007). We focus only on the early part of both experiments (10–18-h run time [RT] in XES 02 and 80–100-h RT in the presubsidence stage of XES 05), in which base level did not vary and subsidence rate was zero or very small. The duration of data presented here to illustrate autogenic processes is limited by the amount of time that boundary conditions were steady in each experiment.

Both experimental runs began with a 3-m-long fan delta, prograding over a flat basement (fig. 2). Slight forehinge-style subsidence was imposed in the XES 02 experiment. During the 8-h period of analysis in XES 02, relative base level increased by 25 mm at the shoreline position; thus, the water depth at the shoreline was around 125 mm at 18 h RT. Experiment XES 05 employed a very shallow standing body of water (water depth = 5 mm), with no change in relative base level.

Data Collection

Data collection methods for the XES 02 and XES 05 experiments were described previously (Paola 2000; Cazanacli et al. 2002; Sheets et al. 2002; Hickson

Table 1. Experimental Parameters in Experiments XES 02 and XES 05

	XES 02	XES 05
Sediment and water supply:		
Sediment supply Q_s (m^3/h)	.0182	.0035
Water supply Q_w (m^3/h)	1.5	.35
Ratio Q_s/Q_w	.012	.01
Sediment mixture (fraction/grain size):		
Quartz sand (%/μm)	63/110	70/110
Coal sand (%/μm)	27/(bimodal 460 and 190)	30/(bimodal 460 and 190)
Kaolinite (%)	10	0

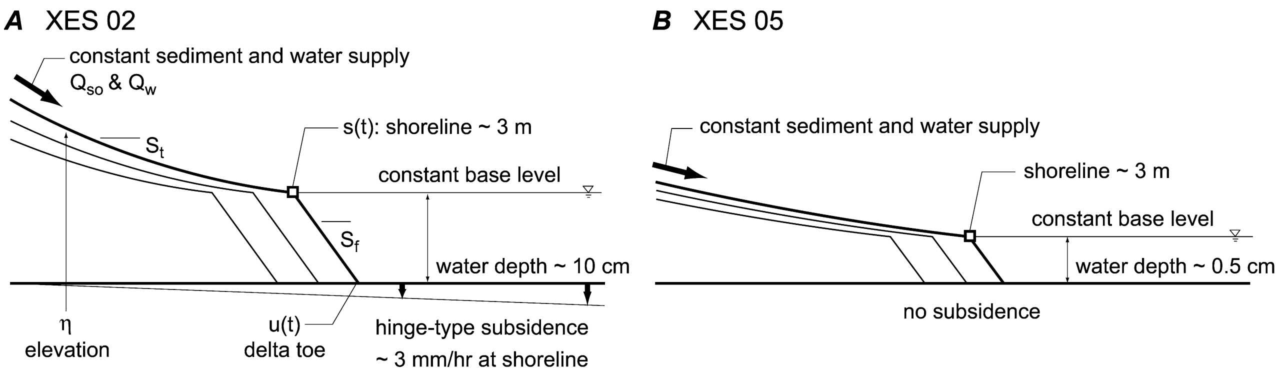

Figure 2. Experimental settings for stages with a constant base level in XES 02 (*A*) and XES 05 (*B*). Deeper water depth (~10 cm) and slight fore-tilting subsidence are present in XES 02, whereas shallow water depth (~0.5 cm) and no subsidence are present in XES 05.

et al. 2005; Strong et al. 2005; Kim et al. 2006*a*, 2006*b*) and so are briefly outlined here. The primary data used for the present analysis consist of overhead images of the fan delta, taken every 2 min for XES 02 and every 1 min for XES 05. For visualization purposes, water was dyed blue and made opaque by adding titanium dioxide, and images were converted to grayscale maps of flow depth (fig. 1*B*), using dye intensity as a proxy for water depth (Kim et al. 2006*a*; Kim and Paola 2007). The wetted perimeter and shoreline were then automatically extracted from each image. Data products derived from this process were time series of wet fraction (the fractional area covered by water) and mean shoreline position for each experiment (fig. 3).

In addition, topographic scans were performed using a laser sheet system and an ultrasonic sonar transducer that allows topographic grid data of both the delta topset and submerged delta foreset with a horizontal resolution of 50 mm in depositional dip direction and 10 mm in strike direction and with a submillimeter vertical resolution (fig. 4). The frequency of the surface scans was limited because experiments had to be paused for the duration of surface topography measurement; hence, scans were taken every 4–8 h in XES 02 and every 2.5 h in XES 05. Topographic maps provide high spatial-resolution data but low temporal-resolution data on the slope and roughness of the surface.

After each experiment, the final deposit was sliced and digitally imaged, as described previously (Heller et al. 2001; Sheets et al. 2002; Hickson et al. 2005; Strong et al. 2005; Kim et al. 2006*a*, 2006*b*). The result is an image scan that is similar to a seismic survey but has a resolution comparable to the scale of individual sand grains (~200 μm; fig. 5). Submerged deposit thickness for XES 05 was very small due to the shallow water depth (5 mm), so subsurface architecture representing foreset accretion could not be clearly assessed for this run. Stratigraphic data analyzed here are confined to XES 02, where subsequent slow base-level change (i.e., relatively longer timescale perturbation than that of the system response time) and high sediment discharge allowed for high-quality preservation of the stratigraphic record that we analyze here (Kim et al. 2006*b*).

Experimental Results

Fluvial Pattern Change and Shoreline Regression. As a result of the imposed boundary conditions, the overall direction for shoreline migration was seaward for both experiments. Mean shoreline position should increase as the square root of time for an extending fluvial surface fed by a constant sediment supply (Muto and Swenson 2005; Kim et al. 2006*a*; Kim and Muto 2007). In order to examine variability in shoreline position, the expected square-root relation was imposed on the data, and this first-order trend was removed (fig. 3*A*, 3*C*). The result is a time series showing quasi-periodic fluctuations in laterally averaged shoreline position for both experiments. These fluctuations represent sediment storage and release in the fluvial system under steady basin forcing (Kim et al. 2006*a*; Kim and Muto 2007). While the duration of data is not sufficient to rigorously compute the period of these fluctuations, visual inspection (e.g., fig. 3) shows a time difference between storage and release events of 2–3 h for XES 02 and 8–10 h for XES 05.

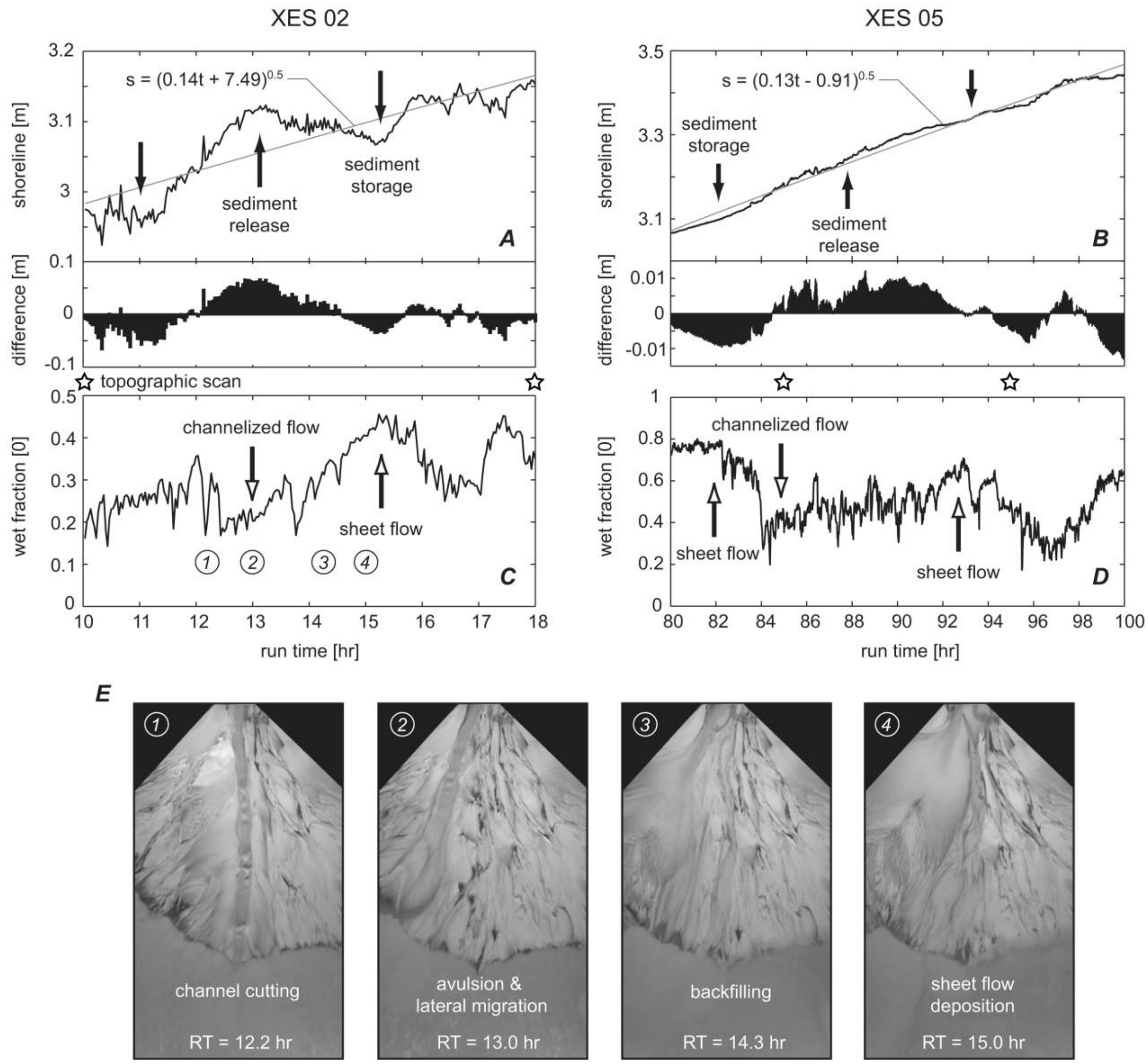

Figure 3. Shoreline and wet-fraction data from XES 02 (*A*, *C*) and 05 (*B*, *D*). *A*, *B*, Mean shoreline position averaged normal to the mean sediment transport direction and best fit curves. Graphs show shoreline position fluctuations after removal of long-term shoreline regression trend. *C*, *D*, Time series of wet fraction showing cyclic changes in fluvial pattern between sheet and channelized flow. *E*, Representative overhead images showing a cycle of wet-fraction change: (1) channel cutting and flow focusing, (2) channel avulsion and lateral migration, (3) backfilling, and (4) sheet flow deposition. Time of each image is indicated in *C*. A color version of this figure is in the online edition of the *Journal of Geology*.

Even more striking than the observed fluctuations in shoreline position is the time-varying nature of flow width, as measured by the wet fraction (fig. 3*C*, 3*D*). Fluvial flow pattern alternated between primarily sheet flow (large wet fraction) and largely channelized flow. The wet fraction varied between 15% and 45% over 2–3 h for XES 02 and between 20% and 75% over 8–10 h for XES 05. Changes in flow pattern appeared to coincide with fluctuations in shoreline position (fig. 3*B*, 3*D*). However, we note again that there are not sufficient data to rigorously evaluate this relationship.

The high-resolution images allow us to describe the cycle of wet-fraction variation (fig. 3*E*). An initial sheet or tabular flow style developed a fan-shaped deposit (fig. 4), during which time migration of the shoreline was limited. Generally, a scour hole would initiate at some point on the fan surface and migrate rapidly upstream, focusing the flow into a more channelized pattern. The channelized flow

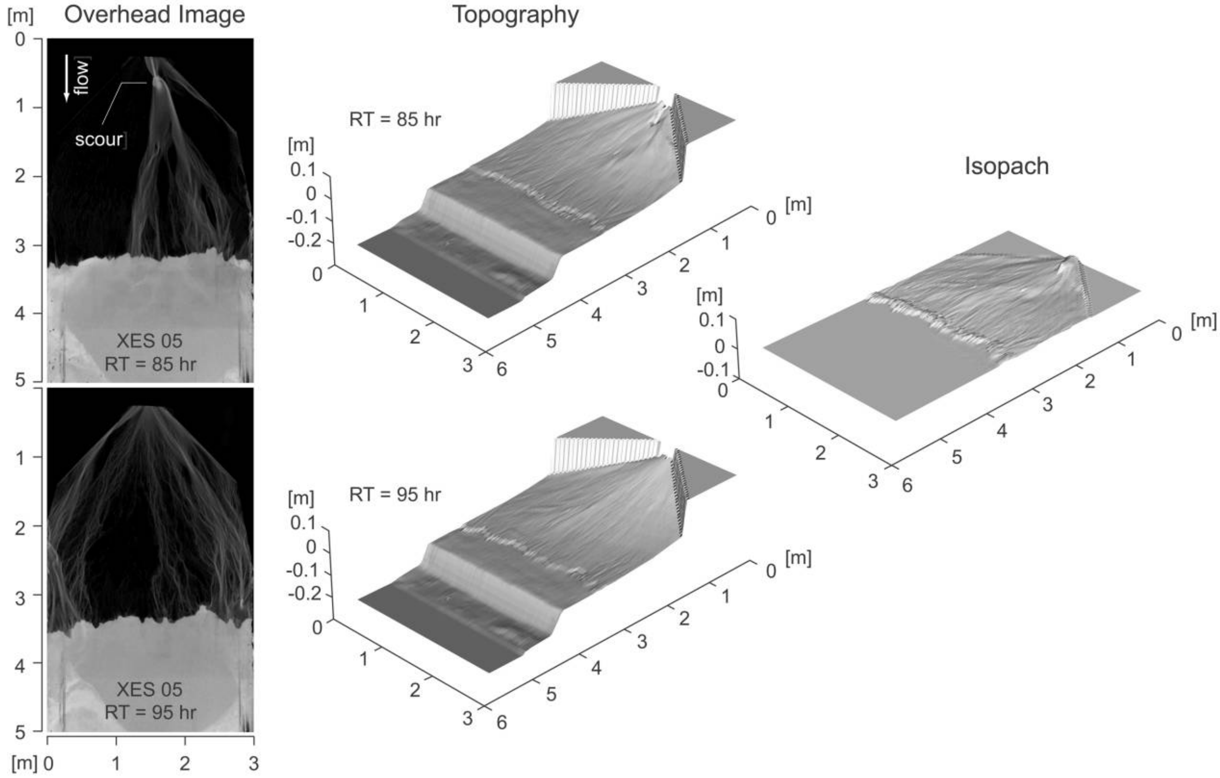

Figure 4. Topographic scan data of run time (RT) = 85 and 95 h in XES 05 and the corresponding flow depth maps. Local depositional pattern is shown in the isopach constructed using two topographic scans given above.

effectively eroded the fluvial surface, delivering sediment to the shoreline. Because of the noncohesive nature of the experimental sediment mixture, newly formed channels migrated rapidly across the delta topset, reworking the entire fluvial surface. Shoreline regression was most pronounced when channelized flow was cutting through a previously developed fan-shaped deposit. Once the surface was reworked, a flow divergence generally developed somewhere downstream on the fan and gradually shifted upstream, backfilling the fluvial surface and returning the flow to a tabular style (fig. 3*E*). During these backfilling episodes, little sediment reached the shoreline. Topographic scans and grayscale flow maps of XES 05 at RT = 85 h and 95 h, respectively, capture both channelized flow and sheet flow and, thus, sediment release and storage processes (fig. 4). Migration of the scour hole shown in the topographic scan and the overhead image at RT = 85 h excavated the fluvial surface and caused a major sediment release event. The topographic roughness due to the scour migration was decreased by flow diversion and sediment backfill. As indicated in both the topographic scans and the isopach between two consecutive scans at RT = 85 and 95 h (fig. 4), the high deposition associated with sheet flow tended to smooth the fluvial surface.

Regular Cyclic Sedimentation in Dip Sections. Large-scale fluctuations in shoreline position reflect changes in the overall transport efficiency of the fluvial system. This variability in transport efficiency is recorded in the stratigraphy as changes in grain-size distribution on the accreting delta foreset. As mentioned, XES 02 was the only experiment to preserve a significant record of deposition during the initial phase of steady boundary conditions. Figure 5 shows a representative dip (X) direction slice of the final deposit in the XES 02 experiment. Image data corresponding to the initial stage of steady experimental controls were extracted (fig. 5*A*), corrected for hinge-type subsidence, and converted to a gray scale to indicate proportion of sand in the deposit (fig. 5*B*). These data are of sufficient length to perform time series analysis of the variation in black (coal; proxy for "fine") and white (quartz; proxy for "coarse") sand deposits in the accreting delta foreset. Autocorrelations were calculated for each of three image slices taken at lateral locations of $Y = 1.9$, 2.1, and 2.3 m and were then ensemble averaged to

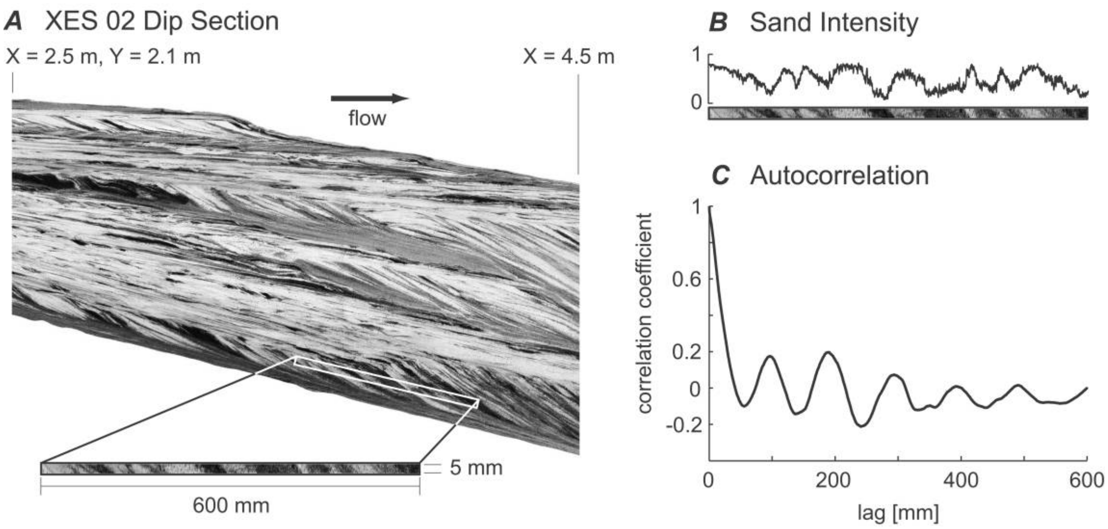

Figure 5. *A*, Representative dip section sliced at $Y = 2.1$ m of the XES 02 final deposit. Data for analyzing the scale of alternation in sand-coal sedimentation were collected at the bottom of the final deposit, where deposits under a stable base-level condition were preserved. *B*, Grayscaled sand intensity. *C*, Autocorrelation of grayscaled sand intensity, averaged from sliced sections at $Y = 1.9$, 2.1, and 2.3 m, indicating a periodic alternation in sand-coal sedimentation with a wavelength of 100 mm.

generate a representative autocorrelation series for the experiment (fig. 5*C*). The analysis clearly indicates regular switching between sand- and coal-dominated deposits with a well-defined wavelength of 100 mm.

Interpretation and Discussion

Boundary conditions for both experiments described here were steady, and therefore, any variability observed in shoreline and wet-fraction dynamics must be the result of the mechanics of sediment transport within the fluvial system. If lateral migration and channel avulsion (i.e., abrupt relocation of established channels) were the only autogenic processes, then strong fluctuation of the laterally averaged shoreline position would not occur. The large fluctuations that are observed (fig. 3) indicate time variation of sediment transport efficiency for the entire fluvial system. Rather than generating spatially variable "local noise," autogenic processes on the delta topset create a coherent, systemwide pulse (Kim et al. 2006*a*). The apparent coincidence of wet-fraction variation and shoreline position is suggestive of a causative relationship, which we explore here through the use of scaling analysis and mathematical modeling.

Timescale and Event Size of Autogenic Processes. Topographic scans in the XES 05 experiment captured delta morphology associated with sheet flow and channelized flow and may therefore be used to estimate the volume of sediment that accounts for shoreline migration events. Slopes of the longitudinally averaged fluvial surface at RT $= 85$ and 95 h were 0.0470 and 0.0497, respectively. The amount of sediment that can be accommodated between these two slopes, assuming linear fluvial profiles, is represented as

$$\Psi_s = 0.5\Delta S_t s^2 B_t, \tag{1}$$

where ΔS_t denotes the difference of minimum and maximum topset fluvial slopes, s is the distance of the shoreline from the delta apex, and B_t denotes the total basin width. For XES 05, the computed fluvial storage volume is $\Psi_s = 0.0318$ m^3. If we assume that all sediment is captured on the delta topset, the time needed to fill the fluvial buffer between two critical release and storage slopes can be written as

$$T_{ap} = \frac{\Psi_s}{Q_{so}}, \tag{2}$$

where T_{ap} denotes the autogenic process timescale and Q_{so} is the sediment discharge input at the apex of the delta, or origin. Equation (2) yields a time of 9.1 h for XES 05, in good agreement with the observed timescales of shoreline fluctuation and change in wet fraction (fig. 3*B*, 3*D*). This simple calculation verifies that systemwide changes in fluvial slope are related to shoreline pulsing, and it implicates flow width variation as well.

During the sediment release process, channels excavate the fluvial storage, and the surface slope cuts down to the minimum critical slope for the release event, 0.0470 in the case of XES 05. The nonlinearity of sediment transport is such that for the same flow discharge, a relatively narrow and deep channel requires a much lower slope for transport compared to the sheet flow case (Paola 1996; Parker et al. 1998; Whipple et al. 1998); hence, reduction in flow width should cause a reduction in slope for the channelized portion. Avulsion and/or lateral migration of channels may then regrade the entire fluvial surface to achieve the channelized slope (Parker et al. 1998). Fluvial erosion causes high sediment discharge at the shoreline, inducing shoreline regression (fig. 6). The distance of shoreline translation by a release event, Λ, is related to the associated change in fluvial slope through conservation of mass at the shoreline:

$$\frac{S_{\mathrm{ch}}}{2H_{\mathrm{f}}}(\Lambda + s)^2 + \Lambda = \frac{(S_{\mathrm{ch}} + \Delta S_{\mathrm{t}})}{2H_{\mathrm{f}}} s^2, \tag{3}$$

where S_{ch} denotes the fluvial slope for a system with channelized flow and H_{f} denotes the toe depth, that is, the elevation difference between the base level and the delta toe (fig. 6). Using the experimental parameters for XES 05 (i.e., $S_{\mathrm{ch}} = 0.0470$, $H_{\mathrm{f}} = 0.005$ m, $\Delta S_{\mathrm{t}} = 0.0027$, and $s = 3.3$ m), the shoreline regression distance caused by a release event is 91 mm, which is consistent with the total shoreline regression during the sediment release period (e.g., RT = ~85–~90 h) shown in figure 3*B*.

We cannot perform the same calculations for XES 02, as the change in fluvial slope is unknown due to insufficient topographic data. We may use the available stratigraphic data, however, to infer the magnitude of this slope change. The distance of shoreline translation associated with a sediment release event is equal to the wavelength of grain-size variation of the deposit (fig. 5), that is, $\Lambda \cong 100$ mm. Setting $S_{\mathrm{ch}} = 0.036$ (the mean fluvial slope from the topographic scan taken at RT = 18 h) and using equation (3), it is found that the associated slope change should be $\Delta S_{\mathrm{t}} = 0.004$. This fluvial buffer would store $\Psi_{\mathrm{s}} = 0.0456$ m^3 of sediment, with a timescale T_{ap} of 2.5 h at the given sediment supply rate. This is in good agreement with the time series of shoreline position and wet fraction for XES 02 (fig. 3), which show a fluctuation timescale of 2–3 h.

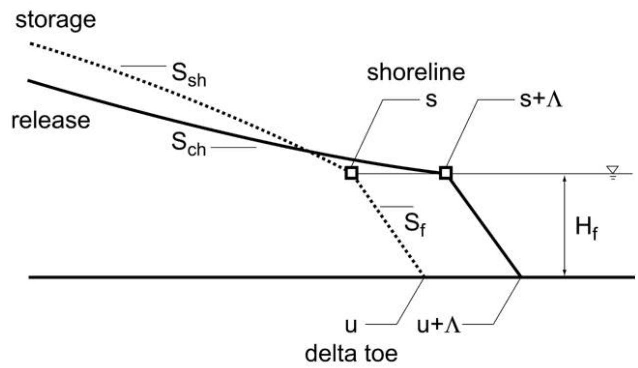

Figure 6. Fan delta downstream profiles at maximum sediment storage and release events. Two profiles contain the same amount of sediment under the surface; difference in shoreline position is caused by the change in fluvial slopes for storage and release stages.

Modeling Variation in Flow Pattern—Equilibrium Model. We have documented large-scale fluctuations in shoreline position, which may be explained by cyclic variation in the fluvial slope (Kim et al. 2006*a*). Where topographic scans were available (i.e., XES 05), we verified that the observed change in fluvial slope is consistent with the volume of sediment required to generate shoreline migration pulses. The experimental data indicate a temporal correlation between flow width (wet fraction) and shoreline migration rate, suggesting that storage and release of sediment in the fluvial buffer corresponds to alternation between sheet flow and channelized flow. Here we examine this connection mechanistically, using a one-dimensional model for the evolution of a fan delta profile.

We begin with the Parker et al. (1998) formulation for a steady state alluvial fan but modify the model for the case of a delta undergoing both fluvial and foreset sedimentation. Details of the model and its derivation can be found in the appendix, available in the online edition or from the *Journal of Geology* office. We assume that no sediment escapes beyond the delta toe and that the delta foreset has a prescribed, linear geometry sloping with a constant slope S_{f} (fig. 6). With the appropriate boundary conditions, we may derive an equation for the shoreline migration rate as a consequence of mass conservation (see appendix). As discussed by Whipple et al. (1998), flows on experimental noncohesive fans are not fully channelized, and so modeling using partial sheet flow parameters is more appropriate. The active flow width is defined as a fraction χ of aerial coverage of sheet flow multiplied by the total basin width, $B_{\mathrm{ch}} = \chi B_{\mathrm{t}}$, where χ is a constant value between 0 and 1. The goal of our modeling exercise is not to tune parameters to maximize agreement with the experiment but rather to gain fundamental insight into the nature of deltaic evolution. For this reason, all coefficients and exponents of the model are chosen following those outlined for a sand bed system by Parker et al. (1998; appendix). Using the observed mean wet fraction, the computed equilibrium slopes are 0.037 and 0.070 for the XES 02 and XES 05 experiments, respectively, while the measured slopes are 0.036 and 0.048. Agreement between experimental and theoretical slope values is very good for XES 02 and decent for XES 05, verifying that the model provides a reasonable description of mean delta geometry.

Using equation (A5) (appendix), we can compute the average fan slope that should result from flow conditions associated with different wet fractions. For XES 02, the wet fraction fluctuated between $\chi = 0.15$ and $\chi = 0.45$; the corresponding average slopes would be 0.028 and 0.043, respectively, giving $\Delta S_t = 0.015$. While slope difference was not measured directly in the experiment, the slope difference required to generate the observed shoreline pulses is $\Delta S_t = 0.004$. Thus, the equilibrium fan model using the minimum and maximum wet-fraction values overestimates slope fluctuations by a factor of 4. For XES 05, the comparison is even worse; the computed slope difference based on a minimum and maximum wet fraction of $\chi = 0.20$ and $\chi = 0.75$, respectively, is $\Delta S_t = 0.034$, while the observed slope change was much smaller, $\Delta S_t = 0.003$. What is missing in this formulation?

Modeling Variation in Flow Pattern—Dynamic Model. The problem with the described model lies in the assumption of equilibrium on the fan surface. The computed minimum and maximum slopes based on wet-fraction values assume that the fluvial slope achieves instantaneous equilibrium with the imposed flow width. In reality, the fluvial surface has a response time that is dictated by the size of the delta and the mean sediment transport rate (Paola et al. 1992; Paola 2000). This equilibrium time is the so-called diffusion timescale,

$$T_{eq} = \frac{L^2}{\nu}, \tag{4}$$

where L is a representative fluvial length scale of the system, $\nu = Q_{so}/(B_t \overline{S}_t)$ is fluvial diffusivity, and $\overline{S}_t$ is the average fluvial slope. Using mean values for XES 02 and XES 05, computed basin equilibrium times are $T_{eq} \cong 60$ h ($L = 3$ m, $Q_{so} = 0.018$ m^3/h, $B_t = 3$ m, and $S_t = 0.04$) and $T_{eq} \cong 390$ h ($L = 3$ m, $Q_{so} = 3.5 \times 10^{-3}$ m^3/h, $B_t = 3$ m, and $S_t = 0.05$), respectively. For comparison, the peak-to-peak period of wet-fraction variation for each experiment, T_b, is 5 and 12 h, respectively (fig. 3). Thus, wet fraction varies on a timescale that is significantly shorter than the equilibrium time of the system ($T_b \ll T_{eq}$), and we therefore expect slope fluctuations to be damped, compared with those values predicted by the equilibrium model.

To test this idea, we investigate the dynamic response of the fluvial slope to a time-varying input of flow width using a variant on the equilibrium model outlined above and input parameters from the XES 02 and XES 05 experiments (see appendix). We represent wet-fraction variation as an idealized sine wave with a specified period, T_b (fig. 7), and impose this time-varying flow width on the entire fluvial profile. We then solve the sediment transport and conservation of mass equations at successive time steps using the updated flow width to model the time evolution of the fluvial profile.

Using parameters from XES 02, including a wet-fraction variation period $T_b = 5$ h, we see that modeled average slope fluctuates with a range $\Delta S_t = 0.005$ (fig. 7), which is very close to the range $\Delta S_t = 0.004$ that accounts for the observed shoreline regression. Modeling XES 05 with $T_b = 12$ h, the predicted slope variation is $\Delta S_t = 0.003$ (fig. 8), while the observed value is $\Delta S_t = 0.003$. By imposing a dynamically varying flow width on the simplified fan evolution model, we obtain variations in fluvial slope that are in very good agreement with experiments. It is important to note that no tuning of the model was performed; all transport parameters were taken directly from the Parker et al. (1998) formulation for a sand bed fan, while boundary conditions and flow-width parameters were derived from the experiments themselves.

The model allows us to explore the effect of changes in the period of wet-fraction variation. When $T_b \ll T_{eq}$, the magnitude of slope variation is far smaller than that predicted from the equilibrium model. Our expectation, based on fluvial response time arguments outlined above, is that the magnitude of slope variability will increase as the period of wet-fraction variation increases. This expectation is borne out in model results (fig. 7). As T_b approaches T_{eq}, the response time of the fluvial system, ΔS_t, approaches the maximum value predicted by the equilibrium model (fig. 7).

Conceptual Model for Sediment Storage and Release. The importance of this dynamic model is that it illustrates how the observed periodic changes in wet fraction can generate sediment storage and release events of the appropriate magnitude to cause measured shoreline pulses. Further, these

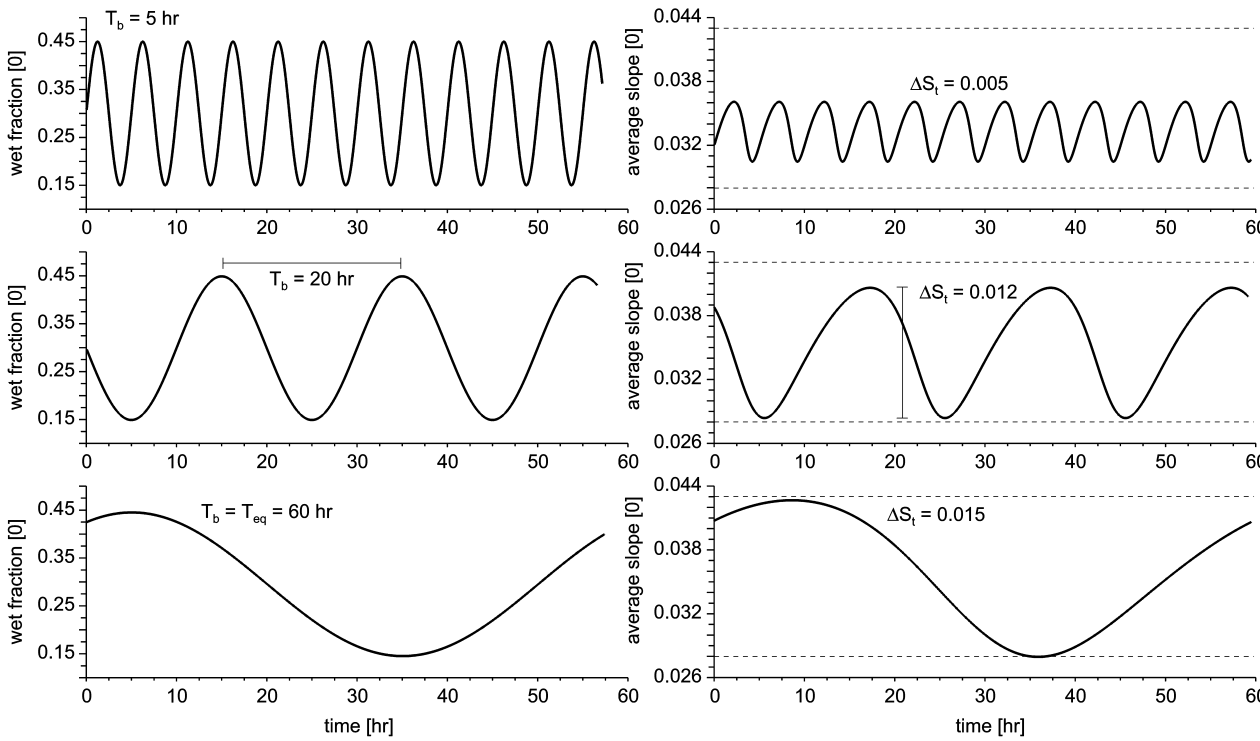

Figure 7. Dynamic model results for XES 02 conditions, showing imposed cycles of wet-fraction variation (*left*) and response of the average fluvial slope to the imposed wet-fraction cycles (*right*). The period of wet-fraction cycles and the amplitude of slope variation are indicated in figure 3; see text for definition of symbols. Dashed lines show minimum and maximum slopes predicted from the equilibrium fan model. The response time of the fan, as computed from equation (4), is also noted.

pulses are recorded as cyclic delta foreset sequences whose thickness also agrees with predicted model results. It is clear that changes in flow width, fluvial slope, and shoreline position are directly related to one another. What has not been addressed in this analysis, however, is the cause of autogenic, periodic changes in wetted width. More fundamentally, the question is what causes transitions in flow style from sheet flow to channelized flow on fans under steady state conditions? This question cannot be resolved from our experimental data or modeling results, but we can propose a conceptual model that is consistent with observations in other systems. Alternation between sheet flow and channelized flow has been observed in other experimental deltas (Schumm et al. 1987; Whipple et al. 1998; Shieh et al. 2001) and also in natural alluvial fans (Blissenbach 1954; Denny 1965; Bull 1977; Hooke and

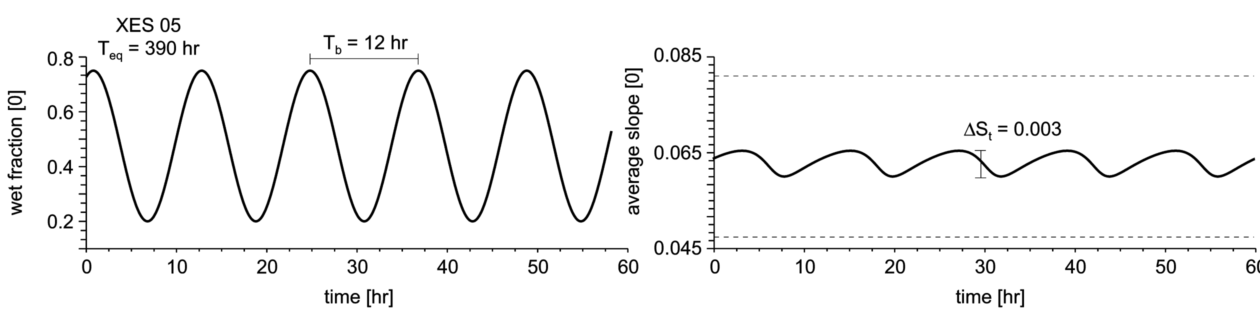

Figure 8. Dynamic model results for XES 05 conditions. *Left*, imposed wet-fraction variation; *right*, response of the average fluvial slope. See the figure 7 legend.

Rohrer 1979; Moore and Nilsen 1984; Blair 1987; Goedhart and Smith 1998) and desert arroyos (Bull 1997), so it appears to be a general phenomenon in unconfined flows over noncohesive sediment.

We conjecture that the instability leading to channel formation on sheet flow fan deltas is the same as the more well-studied case of channel initiation from sheet wash on hillslopes. Theoretical and empirical studies of rill and channel formation on hillslopes have demonstrated that convex surfaces (i.e., positive curvature) are stable to perturbations and resist channelization, while concave surfaces are unstable and tend to channelize and planar surfaces (constant slope) are neutrally stable (Smith and Bretherton 1972; Loewenherz 1991; Montgomery and Dietrich 1992; Loewenherz-Lawrence 1994; Fowler et al. 2007). Mechanistically, the dispersive flow on convex surfaces behaves diffusively (Loewenherz 1991), and thus perturbations to the surface generate a diffusive lateral flux that fills in divots. Concave surfaces allow flow to concentrate, leading to "advective" sediment transport in the sense that down-gradient fluid momentum dominates sediment transport (Loewenherz 1991; Loewenherz-Lawrence 1994). Theory and observation of real hillslopes indicates that channel initiation occurs at the inflection point in the profile, that is, the convex/concave boundary where the slope is maximized. This provides a condition in which to test the hypothesis that channel initiation in the XES experiments is similar to that on hillslopes—channels should initiate at the inflection point in the fluvial profile (Loewenherz 1991). The hillslope analog also suggests that perturbations at the inflection point can migrate upstream as a shock wave (or kinematic wave; Fowler et al. 2007), referred to as a "knick point" in geology, providing another (qualitative) test of the applicability of these models to fan deltas.

Sheet flow conditions in the XES experiments are associated with periods of deposition, which generate increases in both the total slope and the curvature of the fluvial profile (Bull 1977; Parker et al. 1998; fig. 4). Flow entering the apex of the fan becomes unconfined and produces an overall expansion for some distance down the fan. The decrease in flow momentum down the fan that results from this flow expansion is probably responsible for sheet flow sediment deposition. The convexity of the fan surface in our experiments grows with time, having a slope maximum near the middle of the profile, in agreement with theory (Parker et al. 1998). The curvature is not positive everywhere, however. As the fan approaches the downstream boundary (the sea), the slope decreases (both in experiments and in theory [Parker et al. 1998]). Thus, the fluvial profile consists of a convex upper portion, a concave lower portion, and an inflection point that joins the two where slope is maximized (fig. 9). By analogy to the hillslope example, the creation of a substantially large slope at the transition between convex and concave profile segments should initiate a channel head at the inflection point. We mapped the locations on the fan surface where scour holes were initiated, because these scours often migrated headward and led to channel development in the experiment. Data demonstrate that the locations of channel initiation, as defined by the development of scour holes, coincide very well with the point of maximum slope at the inflection in the fluvial profile (fig. 9).

As flow is focused by the initial perturbation, erosion of the fluvial surface occurs that further confines and focuses flow in a positive feedback. The scour holes in the experiments migrated upstream as knick points to create channels, as envisioned by the hillslope model (fig. 9). The flow confinement/erosion feedback may be enhanced by the reduction in flow resistance as depth increases with channelization (e.g., Lawrence 2000). The narrower flow width results in a lower slope over the channelized portion of the fan surface. Lateral channel mobility is high due to the noncohesive nature of the substrate and strong local aggradation of the channel bed near the shoreline, so a fairly large portion of the delta topset is regraded to the lower slope within a relatively short time. Once the entire surface is reworked and the channel elevated by local regression, flow is no longer confined and so diverges to resume a sheet flow pattern.

Experimental observations qualitatively support the application of hillslope channel instability models to fan deltas. A more rigorous comparison would require (1) high-resolution topographic data showing the temporal development of the fluvial surface in the XES experiments through a storage and release cycle and (2) the development of a two-dimensional (or perhaps three-dimensional) transport model for sheet flow on fans. The former is not possible with the current data, while the latter is beyond the scope of this article. The connection between channelization on hillslopes and noncohesive fans seems compelling, however, and warrants further research.

Application to Field Examples. Alternation between sheet flow and channelized flow was observed to occur frequently on the coarse-gravel Emerald Lake fan (Goedhart and Smith 1998), re-

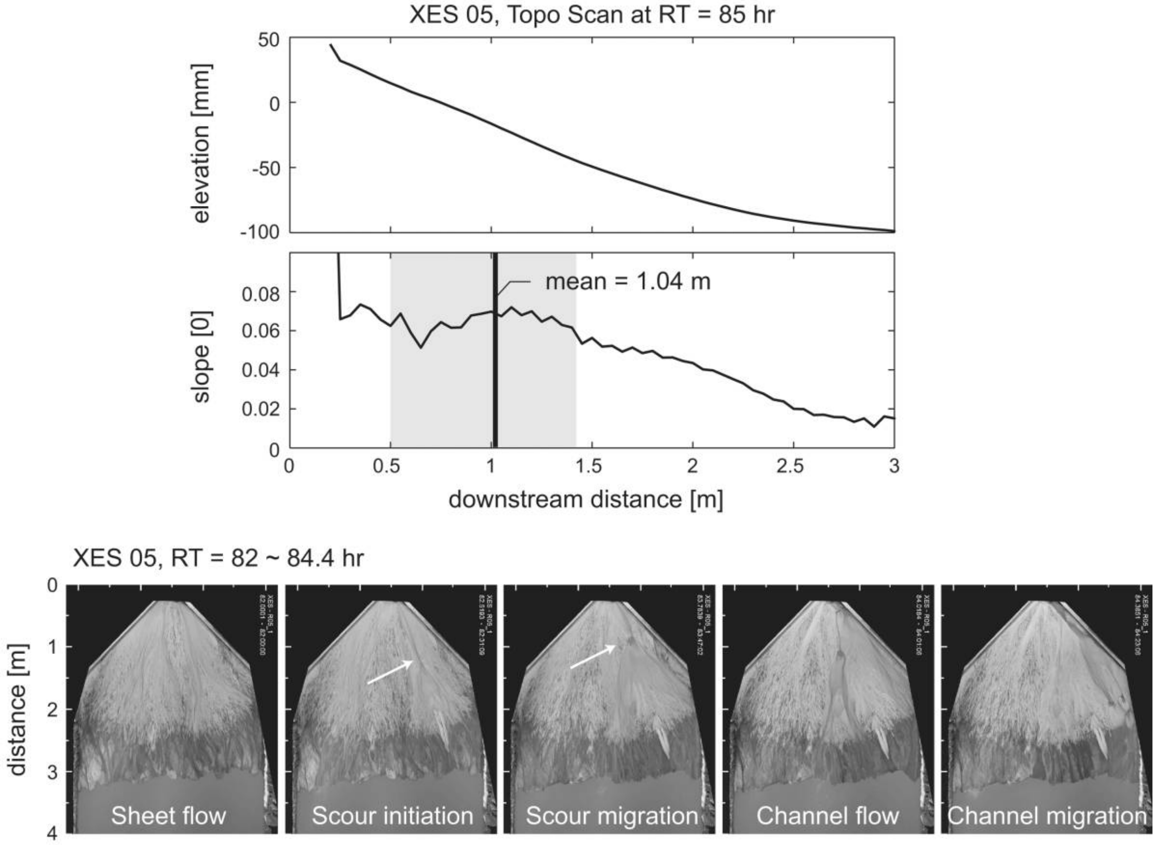

Figure 9. *Top*, cross-stream-averaged fluvial elevation and slope profiles for XES 05 experiment. Topographic scan was taken at run time (RT) = 85 h. Vertical line shows the mean location of scour hole development, which coincides well with the location of maximum slope (except the first ~0.6 m of the fan, where the flow was dominated by inlet effects). The gray shading shows the range of scour hole initiation locations. Scour holes were mapped over the duration 82 h < RT < 87 h using a movie generated from time-lapse images. *Bottom*, sequence of images showing the creation of a scour hole at the fan inflection point and headward migration as a kinematic wave to create a channel. A color version of this figure is in the online edition of the *Journal of Geology*.

sulting in pulsed migration of the fan margin. The striking similarity in flow pattern dynamics suggests that the Emerald Lake fan may be a direct field analog of the XES experiments. More generally, the cycle described above may be common to noncohesive fans in nature and appears also to be strongly related to repeated cut-and-fill cycles described in desert arroyos in the southwestern United States (Bull 1977, 1997). Verification of this idea requires a more detailed, higher-dimensional model and is beyond the scope of this article. It seems reasonable to believe, however, that cyclic parasequences commonly observed in natural fan deltas may well be the result of the described autogenic storage and release processes rather than high-frequency climate or tectonic cycles. To explore this idea, we look at two reported examples of quasi-cyclic Gilbert delta progradation reported in the literature.

Colella (1988) described Gilbert delta deposits that were composed of conglomerate and pebbly sandstone from the Pliocene-Holocene Crati Basin, where the length of the system ranges up to 20 km. Cyclic foreset deposits occur with approximate vertical and horizontal dimensions of 100 m and 400 m, respectively (area $[A = \Psi_s/B_t]$ is approximately $40,000\ m^2$, with all dimensions estimated from sketches). Colella (1988) attributed this pattern to repetitive, large-scale fault slip events. We propose that these depositional cycles may have resulted from autogenic fluctuations in fluvial slope as described above. Using equation (1), foreset parasequences would require changes in the fluvial slope of $\Delta S_t = 0.0002$. If we assume a mean channel slope of $S_t = 0.01$ (a common value for coarse-grained fans), this would represent a 2% fluctuation. Alternatively, by again assuming $S_{ch} = 0.01$ and $H_f = 100$ m, we can use equation (3) to estimate $\Delta S_t = 0.0006$, a 6% change in fluvial slope. Autogenic fluctuations of 2%–6% of the mean slope are well within the range observed in our experiments and in natural river systems (Kim et al. 2006*a*).

Dorsey et al. (1997) reported cyclic progradation packages in Gilbert deltas from the Pliocene Loreto Basin. These fan deltas were composed mainly of gravel and accumulated over a 100,000-yr period of rapid subsidence. Each parasequence is approximately 50 m thick and 2 km long and is separated from the next one by a marine shell bed, indicating hiatuses in sediment delivery followed by rapid progradation. Dating indicates approximately 6000 yr for deposition of each unit. Dorsey et al. (1997) suggested that clustering of earthquakes was a plausible mechanism to generate these parasequences. Assuming all sediment delivered to the fan was deposited on it, we can estimate the sediment flux input to the fan from equation (2): $Q_{so}/B_t \approx 10\ \mathrm{m}^2/\mathrm{yr}$. If we again assume a channel slope of 0.01, fluvial diffusivity becomes 1000 m^2/yr. The total length of the fluvial system is unknown; however, outcrop exposure indicates it is at least 5 km. From equation (4), we compute a minimum basin equilibrium time of 25,000 yr, far longer than the proposed 6000-yr period of earthquake recurrence. It is unlikely that the fluvial system could respond in a coherent fashion to such short-timescale perturbations (Castelltort and van den Driessche 2003). In our view, a more likely explanation for pulses of progradation and intervening hiatuses in foreset deposition is autogenic cut-and-fill cycles resulting from alternation between channelized and sheet flow on the fan topset.

An important question that arises from these field-scale extrapolations is whether changes in fluvial flow pattern actually occur in nature with timescales of thousands of years, as predicted by our hypothesis. Durations of historic records of stream discharge are too short to provide an adequate assessment of the long-term variation in surface flow systems. However, Knox (1985) and Carson et al. (2007) reported data for long-term variations of flood magnitude (up to ~10 k.yr.) in the Upper Mississippi Valley, Wisconsin, and the Uinta Mountains, northeastern Utah, respectively, which were quantified from the bankfull dimensions of abandoned channels preserved on the floodplain. They used the cross-sectional area of subsurface channels to reconstruct bankfull discharge, using a relationship derived from a nearby active gage. The results indicate a periodic variation in bankfull flood with a magnitude change of ±10%–20% from the mean discharge and with a period of ~4000 yr. The authors implicate high-frequency climate change in driving channel variation, as indicated by forest fire cycles with a comparable period. However, the basin equilibrium timescale calculated from the data given by Carson et al. (2007) is ~75,000 yr, indicating that response of the fluvial system to such short-period perturbations should be significantly damped and lagged. Based on the data ($L = 20$ km, $S_t = 0.0005$, $q_s = 2.6\ \mathrm{m}^2/\mathrm{yr}$) and assuming a 5% fluctuation of the fluvial slope to store and release sediment ($\Delta S_t = 0.000025$), the estimated autogenic timescale of storage and release (~$0.5T_b$) using equations (1) and (2) is approximately 2000 yr, close to the observed channel change period. Results suggest an alternative explanation for variation in the subsurface channel geometry, that is, the fluvial autogenic process.

Conclusions

The shoreline migration of a noncohesive experimental fan delta has been found to exhibit periodic pulses under conditions of steady subsidence, base level, and sediment supply. These pulses are correlated with cyclic changes in flow width on the fluvial surface. Large fluctuations in mean shoreline position require temporal variability in transport efficiency of the entire fluvial system. This coherent, autogenic pulse of sediment storage and release on the delta topset is quite different from the more commonly reported localized "noise" associated with autogenic processes such as avulsion, bank erosion, or bed form migration (Bull 1990; Hooke and Redmond 1992; Hooke 1995; Stolum 1996, 1998). The pulse period occurs at timescales far smaller than the basin equilibrium time and is due to the nonlinear threshold process of the channelization instability.

We have used a one-dimensional morphodynamic model for fan delta evolution to demonstrate the relationship between total flow width, fluvial slope, and shoreline migration in the XES experiments. Since alternation between sheet flow and channelized flow has been reported in other experimental deltas (e.g., Schumm et al. 1987; Whipple et al. 1998; Shieh et al. 2001) and also in natural alluvial fans (e.g., Blissenbach 1954; Bull 1977; Blair 1987; Moreno and Romero-Segura 1997; Goedhart and Smith 1998) and desert arroyos (Bull 1997), we believe the derived results to be general. The dynamic model provides a mechanistic explanation for the generation of autogenic stratigraphy and allows for extrapolation to field scales. The model falls short of providing a complete picture of the autogenic cycle, however, because it does not include the fundamental instability that causes flow to transition from a sheetlike pattern to a more channelized regime.

The conceptual model we present to explain this cycle follows from the premise that channel initiation on fan deltas is mechanistically equivalent to that on hillslopes. This model envisions (1) deposition and an increase in fluvial slope during times of developing a convex upward profile by divergent (sheet) flow; (2) exceeding of some critical slope at the transition from the convex upper fan profile to the concave lower profile, which induces a channelization instability leading to incision in the form of a scour hole; (3) focusing of flow during erosion leading to headward migration of the scour and creation of a channel; and (4) a regrading of the delta topset by the channel followed by resumed sheet flow. Further progress in revealing the cause of sediment storage and release requires a more sophisticated model; however, experimental data support the hillslope channel initiation model.

The statistics of sedimentary units created by autogenic processes have generally been characterized as having either an exponential or a fractal distribution of thicknesses (Drummond and Wilkinson 1993, 1996; Rothman et al. 1994; Drummond et al. 1996; Pelletier and Turcotte 1997; Wilkinson et al. 1998; Diedrich and Wilkinson 1999; Gomez et al. 2002; Jerolmack and Sadler 2007). The recognition of a robust mechanism for creating cyclic fan-delta deposits may help to explain their occurrence in nature without calling on changes in external forcing. Further progress in interpreting the history of Earth surface evolution requires recognition that depositional cycles may be the result of the internally generated dynamics of sediment transport. Many classic depositional sequences record the turbulent response of landscapes to the pulse of the earth's climate cycles. It may be that other depositional cycles record the pulse of sediment transport during calm intervals in the earth's history.

ACKNOWLEDGMENTS

This work is supported by the National Center for Earth-surface Dynamics, a Science and Technology Center funded by the Office of Integrative Activities of the National Science Foundation (under EAR-0120914) and the St. Anthony Falls Laboratory Industrial Consortium (Anadarko, Chevron, ConocoPhillips, ExxonMobil, and Japan Oil, Gas and Metals National Corporation). The project benefited from stimulating discussions with C. Paola and G. Parker. We also thank reviewers R. Slingerland and B. Wilkinson for their constructive and substantive comments, which greatly enhanced the quality of this manuscript.

REFERENCES CITED

Allen, P. A., and Densmore, A. L. 2000. Sediment flux from an uplifting fault block: processes and controls in the stratigraphic development of extensional basins. Basin Res. 12:367–380.

Amorosi, A.; Centineo, M. C.; Colalongo, M. L.; and Fiorini, F. 2005. Millennial-scale depositional cycles from the Holocene of the Po Plain, Italy. Mar. Geol. 222–223:7–18.

Blair, T. C. 1987. Tectonic and hydrologic controls on cyclic alluvial-fan, fluvial, and lacustrine rift-basin sedimentation, Jurassic–lowermost Cretaceous Todos Santos Formation, Chiapas, Mexico. J. Sediment. Res. 57:845–862.

Blair, T. C., and Bilodeau, W. L. 1988. Development of tectonic cyclothems in rift, pull-apart, and foreland basins: sedimentary response to episodic tectonism. Geology 16:517–520.

Blissenbach, E. 1954. Geology of alluvial fans in semiarid regions. Geol. Soc. Am. Bull. 65:175–189.

Bull, W. B. 1977. The alluvial fan environment. Prog. Phys. Geogr. 1:222–270.

———. 1990. Stream-terrace genesis: implications for soil development: soils and landscape evolution. Geomorphology 3:351–367.

———. 1997. Discontinuous ephemeral streams. Geomorphology 19:227–276.

Carson, E. C.; Knox, J. C.; and Mickelson, D. M. 2007. Response of bankfull flood magnitudes to Holocene climate change, Uinta Mountains, northeastern Utah. Geol. Soc. Am. Bull. 119:1066–1078.

Castelltort, S., and van den Driessche, J. 2003. How plausible are high-frequency sediment supply–driven cycles in the stratigraphic record? Sediment. Geol. 157:3–13.

Cazanacli, D.; Paola, C.; and Parker, G. 2002. Experimental steep, braided flow: application to flooding risk on fans. J. Hydraul. Eng. 128:322–330.

Colella, A. 1988. Fault-controlled marine Gilbert-type fan deltas. Geology 16:1031–1034.

Cui, Y.; Parker, G.; Pizzuto, J.; and Lisle, T. E. 2003. Sediment pulses in mountain rivers. 2. Comparison between experiments and numerical predictions. Water Resour. Res. 39:1240.

Denny, C. S. 1965. Alluvial fans in the Death Valley region, California and Nevada. U.S. Geol. Surv. Prof. Pap. 466.

Diedrich, N. W., and Wilkinson, B. H. 1999. Depositional cyclicity in the lower Devonian Helderberg group of New York State. J. Geol. 107:643–658.

Dorsey, R. J., and Umhoefer, P. J. 2000. Tectonic and eustatic controls on sequence stratigraphy of the Pliocene Loreto basin, Baja California Sur, Mexico. Geol. Soc. Am. Bull. 112:177–199.

Dorsey, R. J.; Umhoefer, P. J.; and Falk, P. D. 1997. Earthquake clustering inferred from Pliocene Gilbert-type fan deltas in the Loreto Basin, Baja California Sur, Mexico. Geology 25:679–682.

Drummond, C. N., and Wilkinson, B. H. 1993. Aperiodic accumulation of cyclic peritidal carbonate. Geology 21:1023–1026.

———. 1996. Strata thickness frequencies and the prevalence of orderedness in stratigraphic sequences. J. Geol. 104:1–18.

Drummond, C. N.; Wilkinson, B. H.; and Lohmann, K. C. 1996. Climatic control of fluvial-lacustrine cyclicity in the Cretaceous cordilleran foreland basin, western United States. Sedimentology 43:677–689.

Ellis, M. A.; Densmore, A. L.; and Anderson, R. S. 1999. Development of mountainous topography in the Basin and Ranges, USA: thematic set on interactions of tectonics and surface processes in landscape evolution. Basin Res. 11:21–41.

Fowler, A. C.; Kopteva, N.; and Oakley, C. 2007. The formation of river channels. SIAM J. Appl. Math. 67: 1016–1040.

Goedhart, M. L., and Smith, N. D. 1998. Braided stream aggradation on an alluvial fan margin: Emerald Lake fan, British Columbia. Can. J. Earth Sci. 35:534–545.

Gomez, B.; Page, M.; Bak, P.; and Trustrum, N. 2002. Self-organized criticality in layered, lacustrine sediments formed by landsliding. Geology 30:519–522.

Gupta, S.; Underhill, J. R.; Sharp, I. R.; and Gawthorpe, R. L. 1999. Role of fault interactions in controlling synrift sediment dispersal patterns: Miocene, Abu Alaqa Group, Suez Rift, Sinai, Egypt. Basin Res. 11: 167–189.

Haq, B.; Hardenbol, J.; and Vail, P. R. 1987. Chronology of fluctuating sea level since the Triassic (250 million years to present). Science 235:1156–1167.

Heller, P. L.; Paola, C.; Hwang, I.; John, B.; and Steel, R. 2001. Geomorphology and sequence stratigraphy due to slow and rapid base-level changes in an experimental subsiding basin (XES 96-1). Am. Assoc. Petrol. Geol. Bull. 85:817–838.

Hickson, T. A.; Sheets, B. A.; Paola, C.; and Kelberer, M. 2005. Experimental test of tectonic controls on three-dimensional alluvial facies architecture. J. Sediment. Res. 75:710–722.

Hooke, J. M. 1995. River channel adjustment to meander cutoffs on the River Bollin and River Dane, northwest England. Geomorphology 14:235–253.

Hooke, J. M., and Redmond, C. E. 1992. Causes and nature of river planform changes. *In* Billi, P.; Hey, R. P.; Thorne, C. R.; and Tacconi, P., eds. Dynamics of gravel-bed rivers. Hoboken, NJ, Wiley, p. 549–563.

Hooke, R. L., and Rohrer, W. L. 1979. Geometry of alluvial fans: effect of discharge and sediment size. Earth Surf. Proc. 4:147–166.

Howard, A. D. 1982. Equilibrium and time scales in geomorphology: application to sand-bed alluvial streams. Earth Surf. Proc. Land. 7:303–325.

Imbrie, J.; Hays, J. D.; Martinson, D. G.; McIntyre, A.; Mix, A. C.; Moreley, J. J.; Pisias, N. G.; Prell, W. L.; and Shackleton, N. J. 1984. The orbital theory of Pleistocene climate: support from the revised chronology of the d18O record. *In* Berger, A.; Imbrie, J.; Hays, J.; Kukla, G.; and Saltzman, B., eds. Milankovitch and climate. Dordrecht, Reidel, p. 269–306.

Jerolmack, D. J. , and Mohrig, D. 2005. Frozen dynamics of migrating bed forms. Geology 33:57–60.

Jerolmack, D. J., and Paola, C. 2007. Complexity in a cellular model of river avulsion. Geomorphology 91: 259–270.

Jerolmack, D. J., and Sadler, P. 2007. Transience and persistence in the depositional record of continental margins. J. Geophys. Res. 112, doi:10.1029/2006JF000555.

Jervey, M. T. 1988. Quantitative geological modeling of siliciclastic rock sequences and their seismic expression. *In* Wilgus, C. K.; Kendall, C. G. S. C.; Posamentier, H. W.; Ross, C. A.; and Van Wagoner, J. C., eds. Sea-level changes: an integrated approach. SEPM Spec. Publ. 42:47–69.

Kim, W., and Muto, T. 2007. Autogenic response of alluvial-bedrock transition to base-level variation: experiment and theory. J. Geophys. Res. 112, doi: 10.1029/2006JF000561.

Kim, W., and Paola, C. 2007. Long-period cyclic sedimentation with constant tectonic forcing in an experimental relay ramp. Geology 35:331–334.

Kim, W.; Paola, C.; Swenson, J. B.; and Voller, V. R. 2006*a*. Shoreline response to autogenic processes of sediment storage and release in the fluvial system. J. Geophys. Res. 111, doi:10.1029/2006JF000470.

Kim, W.; Paola, C.; Voller, V. R.; and Swenson, J. B. 2006*b*. Experimental measurement of the relative importance of controls on shoreline migration. J. Sediment. Res. 76:270–283.

Knox, J. C. 1985. Responses of floods to Holocene climate change in the upper Mississippi Valley. Quat. Res. 23: 278–300.

Lawrence, D. S. L. 2000. Hydraulic resistance in overland flow during partial and marginal surface inundation: experimental observations and modeling. Water Resour. Res. 36:2381–2393.

Leopold, L. B.; Wolman, M. G.; and Miller, J. P. 1964. Fluvial processes in geomorphology. San Francisco, W. H. Freeman.

Loewenherz, D. S. 1991. Stability and the initiation of channelized surface drainage: a reassessment of the short wavelength limit. J. Geophys. Res. 96:8453–8464.

Loewenherz-Lawrence, D. S. 1994. Hydrodynamic description for advective sediment transport processes

and rill initiation. Water Resour. Res. 30:3203–3212.
Mackin, J. H. 1948. Concept of the graded river. Geol. Soc. Am. Bull. 5:463–511.
Montgomery, D. R., and Dietrich, W. E. 1992. Channel initiation and the problem of landscape scale. Science 255:826–830.
Moore, T. E., and Nilsen, T. H. 1984. Regional variations in the fluvial Upper Devonian and Lower Mississippian(?) Kanayut Conglomerate, Brooks Range, Alaska: fluvial sedimentation and related tectonic framework, western North America. Sediment. Geol. 38:465–497.
Moreno, C., and Romero-Segura, M. J. 1997. The development of small-scale alluvial fans at the base of a modern coastal cliff: process, observations and implications. Geomorphology 18:101–118.
Muto, T., and Swenson, J. B. 2005. Large-scale fluvial grade as a nonequilibrium state in linked depositional systems: theory and experiment. J. Geophys. Res. 110, doi:10.1029/2005JF000284.
Paola, C. 1996. Incoherent structure: turbulence as a metaphor for braiding. *In* Ashworth, P. J.; Bennett, S. J.; Best, J. L.; and McLelland, S. J., eds. Coherent flow structures in open channels. Chichester, Wiley, p. 705–723.
———. 2000. Quantitative models of sedimentary basin filling. Sedimentology 47(suppl.):121–178.
Paola, C., and Borgman, L. E. 1991. Reconstructing random topography from preserved stratification. Sedimentology 38:553–565.
Paola, C.; Heller, P. L.; and Angevine, C. L. 1992. The large-scale dynamics of grain-size variation in alluvial basins. 1. Theory. Basin Res. 4:73–90.
Paola, C.; Mullin, J.; Ellis, C.; Mohrig, D. C.; Swenson, J. B.; Parker, G. S.; Hickson, T.; et al. 2001. Experimental stratigraphy. GSA Today 11:4–9.
Parker, G.; Paola, C.; Whipple, K. X.; and Mohrig, D. 1998. Alluvial fans formed by channelized fluvial and sheet flow. I. Theory. J. Hydraulic Eng. 124:985–995.
Pelletier, J. D., and Turcotte, D. L. 1997. Synthetic stratigraphy with a stochastic diffusion model of fluvial sedimentation. J. Sediment. Res. 67:1060–1067.
Pitman, W. C. 1978. Relationship between eustacy and stratigraphic sequences of passive margins. Geol. Soc. Am. Bull. 89:1389–1403.
Posamentier, H. W.; Jervey, M. T.; and Vail, P. R. 1988. Eustatic controls on clastic deposition. I. Conceptual framework. *In* Wilgus, C. K.; Hastings, B. S.; Kendall, C. G. S. C.; Posamentier, H. W.; Ross, C. A.; and Van Wagoner, J. C. Sea-level changes: an integrated approach. SEPM Spec. Publ. 42:125–154.
Price, S. P., and Scott, B. 1991. Pliocene Burdur basin, SW Turkey: tectonics, seismicity and sedimentation. J. Geol. Soc. Lond. 148:345–354.
Rothman, D. H.; Grotzinger, J. P.; and Flemmings, P. 1994. Scaling in turbidite deposition. J. Sediment. Res. 64: 59–67.
Sadler, P. M., and Strauss, D. J. 1990. Estimation of completeness of stratigraphical sections using empirical data and theoretical models. J. Geol. Soc. Lond. 147:471–485.
Schumm, S. A.; Mosley, M. P.; and Weaver, W. E. 1987. Experimental fluvial geomorphology. New York, Wiley.
Sheets, B. A.; Hickson, T. A.; and Paola, C. 2002. Assembling the stratigraphic record: depositional patterns and time-scales in an experimental alluvial basin. Basin Res. 14:287–301.
Shieh, C. L.; Tseng, C. M.; and Hsu, S. M. 2001. Development and geometric similarity of alluvial deltas. J. Hydraul. Eng. 127:17–29.
Smith, G. A. 1994. Climatic influences on continental deposition during late-stage filling of an extensional basin, southeastern Arizona. Geol. Soc. Am. Bull. 106: 1212–1228.
Smith, T., and Bretherton, F. P. 1972. Stability and conservation of mass in drainage basin evolution. Water Resour. Res. 8:1506–1529.
Stolum, H. 1996. River meandering as a self-organization process. Science 271:1710–1713.
———. 1998. Planform geometry and dynamics of meandering rivers. Geol. Soc. Am. Bull. 110:1485–1498.
Strong, N.; Sheets, B. A.; Hickson, T. A.; and Paola, C. 2005. A mass-balance framework for quantifying downstream changes in fluvial architecture. *In* Blum, M. D.; Marriott, S. B.; and Leclair, S. F., eds. Fluvial sedimentology. Vol. VII. Spec. Publ. Int. Assoc. Sedimentol. 35:243–253.
Swenson, J. B. 2005. Fluviodeltaic response to sea level perturbations; amplitude and timing of shoreline translation and coastal onlap. J. Geophy. Res. 110, doi:10.1029/2004JF000208.
Whipple, K. X.; Parker, G.; Paola, C.; and Mohrig, D. 1998. Channel dynamics, sediment transport, and the slope of alluvial fans: experimental study. J. Geol. 106: 677–693.
Wilkinson, B. H.; Diedrich, N. W.; Drummond, C. N.; and Rothman, E. D. 1998. Michigan hockey, meteoric precipitation, and rhythmicity of accumulation on peritidal carbonate platforms. Geol. Soc. Am. Bull. 110:1075–1093.